▌**Photochemistry** │*Hot Paper*│

An Iridium(III) Complex as a Photoactivatable Tool for Oxidation of Amyloidogenic Peptides with Subsequent Modulation of Peptide Aggregation

Juhye Kang[+,][a] Shin Jung C. Lee[+,][a] Jung Seung Nam[+,][a] Hyuck Jin Lee,[b] Myeong-Gyun Kang,[a] Kyle J. Korshavn,[c] Hyun-Tak Kim,[a] Jaeheung Cho,[d] Ayyalusamy Ramamoorthy,[c, e] Hyun-Woo Rhee,*[a] Tae-Hyuk Kwon,*[a] and Mi Hee Lim*[a]

Abstract: Aggregates of amyloidogenic peptides are involved in the pathogenesis of several degenerative disorders. Herein, an iridium(III) complex, **Ir-1**, is reported as a chemical tool for oxidizing amyloidogenic peptides upon photoactivation and subsequently modulating their aggregation pathways. **Ir-1** was rationally designed based on multiple characteristics, including 1) photoproperties leading to excitation by low-energy radiation; 2) generation of reactive oxygen species responsible for peptide oxidation upon photoactivation under mild conditions; and 3) relatively easy incorporation of a ligand on the Ir[III] center for specific interactions with amyloidogenic peptides. Biochemical and bio- physical investigations illuminate that the oxidation of repre- sentative amyloidogenic peptides (i.e., amyloid-β, α-synu- clein, and human islet amyloid polypeptide) is promoted by light-activated **Ir-1**, which alters the conformations and ag- gregation pathways of the peptides. Additionally, their po- tential oxidation sites are identified as methionine, histidine, or tyrosine residues. Overall, our studies on **Ir-1** demonstrate the feasibility of devising metal complexes as chemical tools suitable for elucidating the nature of amyloidogenic pep- tides at the molecular level, as well as controlling their ag- gregation.

Introduction

Amyloidogenic peptides are found in human degenerative dis- eases [e.g., amyloid-β (Aβ) for Alzheimer's disease, α-synuclein (α-Syn) for Parkinson's disease, and human islet amyloid poly-

[a] J. Kang,[+] Dr. S. J. C. Lee,[+] J. S. Nam,[+] M.-G. Kang, H.-T. Kim, Prof. Dr. H.-W. Rhee, Prof. Dr. T.-H. Kwon, Prof. Dr. M. H. Lim
Department of Chemistry
Ulsan National Institute of Science and Technology (UNIST)
Ulsan 44919 (Republic of Korea)
E-mail: rhee@unist.ac.kr
kwon90@unist.ac.kr
mhlim@unist.ac.kr

[b] Dr. H. J. Lee
School of Life Sciences, UNIST
Ulsan 44919 (Republic of Korea)

[c] K. J. Korshavn, Prof. Dr. A. Ramamoorthy
Department of Chemistry, University of Michigan
Ann Arbor, MI 48109 (USA)

[d] Prof. Dr. J. Cho
Department of Emerging Materials Science
Daegu Gyeongbuk Institute of Science and Technology (DGIST)
Daegu 42988 (Republic of Korea)

[e] Prof. Dr. A. Ramamoorthy
Biophysics, University of Michigan
Ann Arbor, MI 48109 (USA)

[+] These authors contributed equally to this work.

▭ Supporting information and ORCID number from the author for this article
can be found under:
http://dx.doi.org/10.1002/chem.201604751.

peptide (hIAPP) for type II diabetes].[1] Amyloidogenic peptides have aggregate-prone properties to form β-strand fibrils through oligomeric conformations, and their aggregation has been suggested to be linked to the pathogenesis of degenera- tive disorders.[1] Thus, a variety of approaches have been devel- oped to regulate or suppress the aggregation pathways of amyloidogenic peptides.[1b, 2] Among such methods, peptide modifications, including peptide oxidation, have been recently implicated as a strategy suitable for modulation of amyloido- genic peptide aggregation (Figure 1a).[3]

To trigger the oxidation of peptides, some chemical re- agents, such as metal ions, have been utilized.[3b, 4] Metal ions are frequently used for peptide oxidation; however, they re- quire harsh additional oxidants.[3b, 4] In addition, chemical re- agents capable of generating oxidants from O₂ upon photoac- tivation have been developed for use as photosensitizers in various fields because light is a readily accessible resource.[3a, 5] A series of organic molecules, such as riboflavin, rose bengal, methylene blue, and porphyrins, have been used as photoin- duced reagents;[3a, 5b–h] however, 1) many of them have relative- ly lower quantum yields than those of photoactivatable transi- tion-metal complexes;[6] and 2) some organic agents are less stable, which potentially indicates their degradation upon irra- diation.[5a, i] Photoactivatable metal complexes present relatively high quantum yields, structural stability, and tunable geome- tries and properties upon ligand substitution.[5a, i] Due to these beneficial aspects, multiple metal complexes have been de-
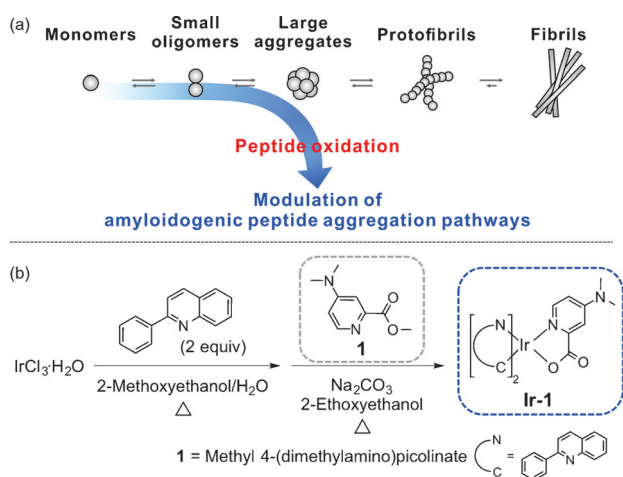
Figure 1. Schematic description of amyloidogenic peptide aggregation and chemical structures of **Ir-1** and **1**. As shown in (a), oxidation of amyloidogenic peptides could control their aggregation pathways. (b) Synthetic routes to **Ir-1**.

signed and mediated for photoinduced oxidation of peptides.[5j–m] One inorganic complex, [Ru(bpy)$_3$]$^{2+}$ (bpy = 2,2′-bipyridine), has been frequently employed for oxidative modifications of peptides through light exposure.[5k–m] To achieve peptide oxidation, however, this ruthenium(II) complex still needs an additional electron acceptor (e.g., ammonium persulfate), which could lead to cytotoxicity and limit its applications.[5k–m, 7] Thus, robust inorganic complexes able to efficiently oxidize peptides simply by light introduction without the assistance of harsh additives would be of significant value for gaining a greater understanding of peptide-related chemistry and biology.

Herein, we report an iridium(III) complex, **Ir-1** (Figure 1 b), as a chemical tool for the oxidation of amyloidogenic peptides with subsequent control of their aggregation under mild conditions that only include readily available O$_2$ and visible light. **Ir-1** was rationally designed as such a tool through incorporating the general properties of Ir^{III} complexes previously reported for various applications, including photoactivation, formation of reactive oxygen species (ROS) upon light exposure, and relatively stable octahedral geometry, as well as relatively easy introduction of a ligand containing a structural moiety, suggested to be important for interactions with amyloidogenic peptides, on the Ir^{III} center.[5a, 8] Representative amyloidogenic peptides (i.e., Aβ, α-Syn, and hIAPP) were indicated to be noticeably oxidized upon treatment of **Ir-1** with photoactivation under aerobic conditions, as monitored by electrospray ionization mass spectrometry (ESI-MS), and their oxidation sites (as potential sites, methionine, histidine, and tyrosine residues) were identified by tandem MS (ESI-MS^2). Even with oxidative modifications of a few residues in these amyloidogenic peptides, the aggregation pathways were noticeably modulated, resulting in distinct morphological features (e.g., smaller-sized or amorphous peptide species, instead of fibrils). Taken together, our rational design and investigations into **Ir-1** illustrate the potential of transition metal complexes as chemical tools for the oxidative modification of amyloidogenic peptides simply

by employing light and O$_2$. In addition, our studies corroborate that small changes in amyloidogenic peptides, such as oxidation at a few specific residues, are able to transform overall peptide aggregation pathways; this suggests novel and viable directions for amyloid management (Figure 1 a).

Results and Discussion

Rational design of Ir-1 for oxidation of amyloidogenic peptides

For the oxidation of amyloidogenic peptides simply upon photoactivation under mild conditions, **Ir-1** (Figure 1 b) was rationally designed as a chemical tool by taking into account the characteristics found in previously reported photoactivatable Ir^{III} complexes, as well as specificity for amyloidogenic peptides: 1) photoproperties with relatively low-energy radiation (i.e., visible light);[8d,e] 2) the ability to produce ROS [e.g., singlet oxygen (^{1}O$_2$)] from redundant O$_2$, which is responsible for peptide oxidation, upon photoactivation;[5a, 8c] 3) robust octahedral coordination, which can provide relative structural stability without any structural modifications when light is introduced;[8c] 4) strong spin-orbit coupling of the Ir^{III} center, which could facilitate electronic transitions without the assistance of additional electron acceptors;[8d,e] and 5) incorporation of a ligand (**1**) containing a dimethylamino group, which is suggested to be crucial for interactions with amyloidogenic peptides,[8a,b] onto the Ir^{III} center (Figure 1 b).

Ir-1 was obtained in relatively high yield (ca. 80%) through previously known two-step procedures with slight modifications, as depicted in Figure 1 b.[9] Moreover, **Ir-1** is easily photoactivatable under mild conditions [e.g., excitation with visible light (ε (463 nm) = 5.78 ($\pm$ 0.12) $\times$ 10^3 M^{-1} cm^{-1}; Table S1 in the Supporting Information) and aerobic conditions] as shown by its quantum yield for phosphorescence [Φ_p = 0.41 ($\pm$ 0.02); Table S1 in the Supporting Information]. The ability of **Ir-1** to generate singlet oxygen (^{1}O$_2$) from triplet dioxygen (^{3}O$_2$) was also confirmed by determining the quantum yield of ^{1}O$_2$ [Φ_s = 0.25 ($\pm$ 0.03); Table S1 in the Supporting Information]. Overall, an octahedral Ir^{III} complex, **Ir-1**, was constructed as a photoactivatable tool to oxidize amyloidogenic peptides without the need for harsh conditions through relatively easy synthetic routes with a high yield, and demonstrated to generate oxidants (i.e., ^{1}O$_2$) from readily accessible O$_2$.

Oxidative modifications of amyloidogenic peptides by Ir-1

To investigate whether the oxidation of amyloidogenic peptides by **Ir-1** under aerobic conditions would occur with light activation, three amyloidogenic peptides (i.e., Aβ, α-Syn, and hIAPP found in Alzheimer's disease, Parkinson's disease, and type II diabetes, respectively) were chosen as representative amyloidogenic peptides, and the resultant monomeric peptide species upon treatment with **Ir-1** were first monitored by means of ESI-MS (Figure 2). These three amyloidogenic peptides were observed to be oxidized with the addition of light-activated **Ir-1** under aerobic conditions. Without light, even in
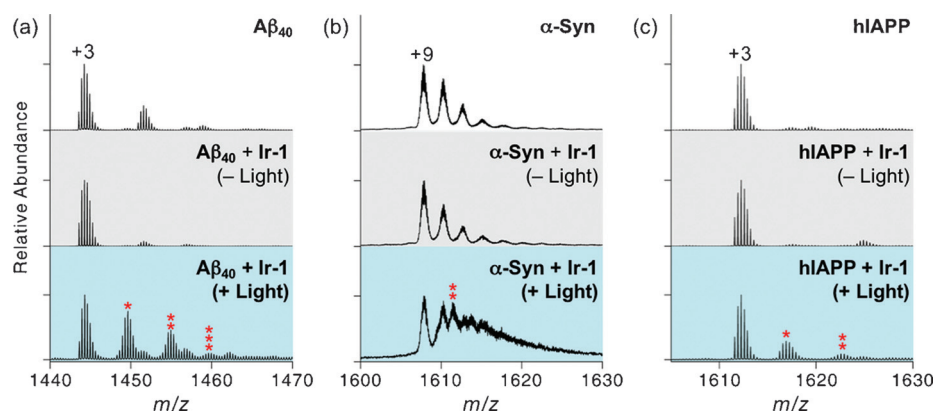
Figure 2. Oxidation of amyloidogenic peptides by **Ir-1** upon light activation. Mass spectrometric analyses of amyloidogenic peptides [(a) Aβ_{40}, (b) α-Syn, and (c) hIAPP] upon treatment with **Ir-1** in the presence of light. Oxidized peptide ions are indicated with red asterisks, and the number of asterisks indicates the number of oxygen atoms incorporated into the peptides. Conditions: [peptide] = 100 μM; [**Ir-1**] = 500 μM; pH 7.4; 37 °C; 1 h; no agitation; 1 sun light for 10 min (for samples treated with light); aerobic conditions. Details for the assignment of oxidized peaks are included in the Experimental Section.

the presence of **Ir-1**, all amyloidogenic peptides were in non-oxidized forms (Figure 2, middle, gray). In the case of Aβ_{40}, the oxidized Aβ monomers had a 16 Da increase in mass from nonoxidized peptides; this implied the incorporation of one oxygen atom into the peptide (Figure 2a, bottom, blue). Notably, ligand **1** alone was not able to oxidize Aβ_{40} (Figure S1 in the Supporting Information). Similar to Aβ_{40}, doubly oxidized α-Syn with a 32 Da increase in mass, relative to that of the native peptide, was indicated; this suggested the introduction of two oxygen atoms into the peptide (Figure 2b, bottom,

Figure 3. Oxidation of Aβ_{40} dimers by **Ir-1** upon photoactivation. (a) ESI-MS spectra for +5-charged dimers with **Ir-1** in the absence and presence of light. The oxidized dimers are only detected by **Ir-1** with light exposure (bottom, blue). The number of red asterisks indicates the number of oxygen atoms incorporated into Aβ_{40} dimers. (b) ATDs for nonoxidized (top and middle) and tetraoxidized dimers (bottom). Each ion selected for IM-MS analysis is indicated with gray arrows in (a). The oxidized dimer incorporated with four oxygen atoms presents the higher abundance in the distribution with short drift time (bottom) than that of nonoxidized Aβ_{40} (top and middle), which implies that structural compaction can be induced by oxidation. Conditions: [Aβ_{40}] = 100 μM; [**Ir-1**] = 500 μM; pH 7.4; 37 °C; 1 h; no agitation; 1 sun light for 10 min (for samples treated with light); aerobic conditions.

blue). Slightly different from both Aβ and α-Syn, singly oxidized monomeric hIAPP presented a 14 Da difference in mass from nonoxidized peptides (Figure 2c, bottom, blue). A 14 Da increase in mass could result from the addition of one oxygen atom to hIAPP, along with deprotonation.[3a, 5f, 10]

Second, we examined whether amyloidogenic peptide oligomers (focusing on Aβ oligomers) by **Ir-1** could be oxidized with light activation under aerobic conditions. From the samples containing Aβ and **Ir-1** upon exposure to light and O$_2$, the oxidation of both dimers and larger oligomers was revealed (Figure 3a and Figure S2 in the Supporting Information). As demonstrated in Figure 3a, multiple oxygen atoms (e.g., for dimers, up to seven oxygen atoms) were indicated to be incorporated into the oxidized oligomers.

Moreover, structural changes to monomeric and oligomeric peptide species accompanied by oxidation were probed by means of ion mobility mass spectrometry (IM-MS), which enabled to characterize conformations based on the mobility of ions passing through a cell filled with neutral gas.[11] In the case of Aβ monomers, there was no remarkable difference in arrival time distributions (ATDs) between singly oxidized and nonoxidized Aβ_{40} monomers (Figure S3 in the Supporting Information). Distinguishable from Aβ monomers, a change in the IM-MS data of Aβ_{40} dimers upon oxidation was presented at two dominant ATDs, centered at 10.80 and 15.55 ms, respectively (Figure 3b). Nonoxidized Aβ_{40} dimers exhibited greater dominance in the larger ATD, whereas the oxidized dimers had the opposite tendency, which suggested that peptide oxidation could lead to structural compaction in the dimers. Although structural details of oxidized dimers have not been elucidated, their structural compaction might assist in modulating peptide aggregation because previous studies indicated that conformationally compact Aβ species could alter peptide aggregation pathways to form amorphous aggregates.[2b–e]

Furthermore, the oxidation of a nonamyloidogenic structured protein, ubiquitin, was also investigated when **Ir-1** was added with light under aerobic conditions. Ubiquitin was selected as an archetypal structured protein because all secon-
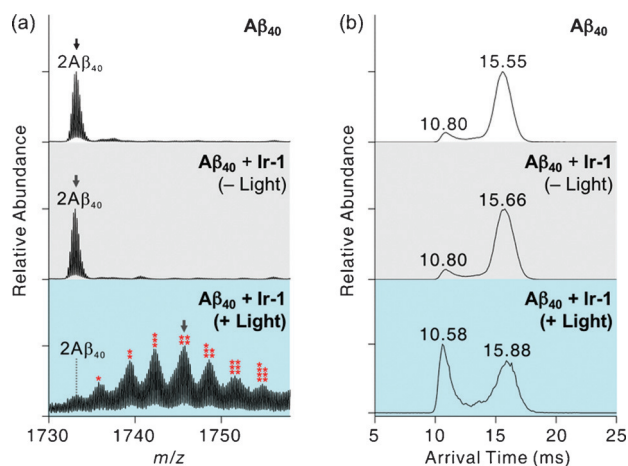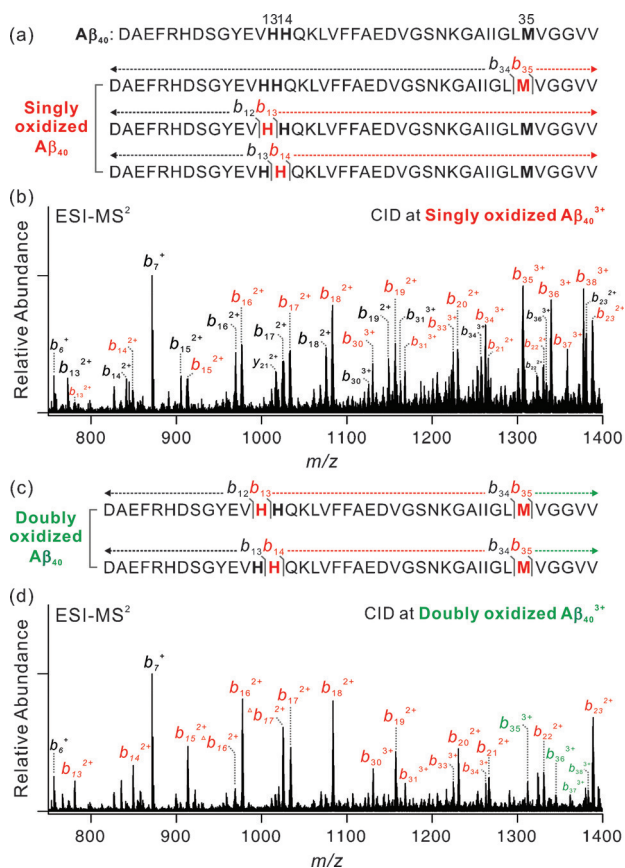
Figure 4. Identification of the oxidation sites in $A\beta_{40}$. (a and c) The peptide sequence and annotation for ESI-MS^2 and (b and d) ESI-MS^2 spectra for singly and doubly oxidized $A\beta_{40}$. Singly and doubly oxidized *b* fragments (N-terminal fragment ions) or *y* fragments (C-terminal fragment ions) are denoted in red and green, respectively. The peaks assigned as triangles (b_{16} and b_{17}) indicate that the loss of a water molecule occurs at serine, threonine, glutamate, or aspartate residues in these fragment ions.[13]

dary structures (e.g., α-helix, β-strand, and random coil) could be found in ubiquitin.[12] Ubiquitin treated with **Ir-1** was shown to be oxidized with light exposure under aerobic conditions (Figure S4 in the Supporting Information, bottom, blue); however, oxidized ubiquitin was significantly less abundant than the oxidized forms of intrinsically disordered amyloidogenic peptides (i.e., $A\beta$, α-Syn, and hIAPP). Overall, oxidative modifications of amyloidogenic peptides, lacking ordered structures, are more readily achieved over structured peptides by **Ir-1** under mild conditions, including light and O_2, which could direct structural compaction; this supports the utilization of **Ir-1** as a photoactivatable tool for the oxidation of amyloidogenic peptides.

Identification of oxidation sites in amyloidogenic peptides

The resultant oxidized amyloidogenic peptides, produced by the addition of **Ir-1** with light exposure under aerobic conditions, were further studied by ESI-MS^2 to determine the oxidation sites in the peptides.[2d,e] The fragment ions generated by selectively applying collisional energy to the singly and doubly oxidized amyloidogenic peptides were analyzed (Figure 4).

First, the oxidation sites in $A\beta_{40}$ were identified. The singly oxidized fragments, highlighted in red, were observed in *b* fragments, which were cleaved from the N-terminus (Figure 4b). All *b* fragments smaller than b_{13} existed as nonoxidized forms, whereas those larger than b_{34} represented only oxidized fragments. Methionine 35 (M35) is known to be the most readily oxidizable amino acid in $A\beta$.[3j] If oxidation occurred only at M35, all fragments smaller than b_{35} would not be oxidized (Figure 4a); however, oxidized *b* fragments were indicated to be smaller than b_{35}, which implied the existence of other oxidation sites (Figure 4b). Based on previously reported studies, other possible oxidation sites could be histidine residues (i.e., H13, H14).[4c, 14] In the ESI-MS^2 spectrum for doubly oxidized $A\beta_{40}$, there was no oxidized fragment smaller than b_{13} (Figure 4d). Because fragments from b_{13} to b_{34} only existed in singly oxidized forms (highlighted in red in Figure 4), this region would include one oxidation site, possibly H13 or H14. All fragments larger than b_{34} were doubly oxidized (denoted in green), which implied the incorporation of one oxygen atom into M35 to generate a sulfoxide form (Figure 4c and d).

For further analysis of the oxidation sites in $A\beta$, $A\beta_{40}$ treated with **Ir-1** in the absence and presence of light was evaluated by 2D band-selective optimized flip-angle short transient heteronuclear multiple quantum correlation (SOFAST-HMQC) NMR spectroscopy (Figure 5 and Figure S5 in the Supporting Information). In the absence of light, minimal chemical shift perturbations (CSPs) of uniformly ^{15}N-labeled $A\beta_{40}$ appeared upon incubation with **Ir-1** (Figure 5b), which implied no significant interaction of **Ir-1** with the peptide. Following exposure of the $A\beta$ samples containing **Ir-1** to light, a dramatic increase in the CSPs at V12, D23, and M35 was observed (Figure 5c). A noticeable change in the CSP of M35 suggests that there are interac-
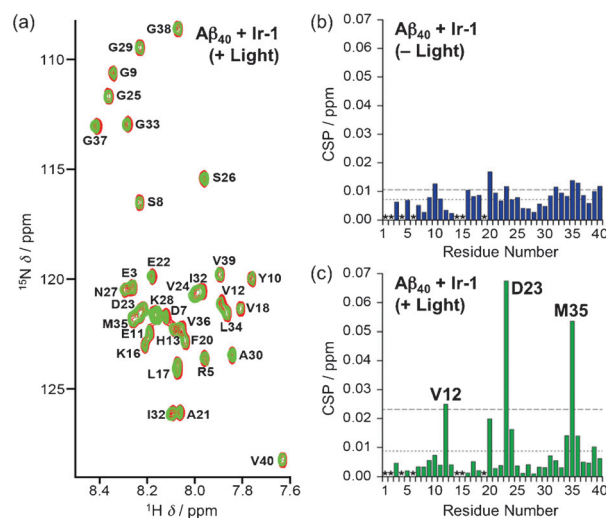

Figure 5. SOFAST-HMQC NMR studies of uniformly ^{15}N-labeled $A\beta_{40}$ monomer upon treatment with **Ir-1** with and without light. (b and c) The chemical shift perturbations (CSPs) for each spectrum [in the absence (Figure S5 in the Supporting Information) or presence of light (a)], relative to the spectrum of $A\beta_{40}$ without **Ir-1**, were calculated. Conditions: [^{15}N-labeled $A\beta_{40}$] = 80 μM; [**Ir-1**] = 160 μM; pH 7.4; 37 °C; ambient light for 1 h (for samples treated with light); aerobic conditions. *Residues could not be resolved for analysis.

tions near M35, which is consistent with observation monitored by ESI-MS^2. In the case of histidine residues, although they were not well resolved within the spectra due to peak overlap, the enhanced CSP of V12, proximately located to H13 or H14, could be expected, which proposed oxidative modifications at H13 or H14, as shown in our ESI-MS^2 studies. Notably, in the NMR spectra, D23 was adjacent to M35 with some overlap, so the shift of M35 might affect its CSP. Thus, our NMR data support that Aβ$_{40}$ is oxidized at specific sites (potentially, M35, H13, and H14) by **Ir-1** upon light stimulation under aerobic conditions.

Potential oxidation sites in the other amyloidogenic peptides (i.e., α-Syn and hIAPP), when treated with **Ir-1** in the presence of light under aerobic conditions, were also investigated by means of ESI-MS^2 (Figure 6). When the collisional energy was applied at doubly oxidized α-Syn (Figure 6 a and b), no oxidation was found in small N-terminal fragments; this reflects that oxidation at M1 and M5 rarely occurs. The C-terminal fragment y_{13} was detected in a nonoxidized form, but b_{119} was present in

both oxidized and nonoxidized forms. One oxidation site existed between P120 and M127, and the most plausible location was M127. Since singly oxidized b_{116} and b_{119} ions were relatively abundant, M116 was also estimated to be possibly oxidized. There were oxidized fragments smaller than b_{116}, such as b_{63}, b_{65}, and b_{66}, which implied that there were oxidation sites other than M116 and M127. Based on our investigations for oxidation sites in Aβ$_{40}$, the histidine residue in α-Syn (i.e., H50) could be an oxidation site. Additionally, in the ESI-MS^2 spectra of singly and doubly oxidized hIAPP (Figure 6 c–e), peptide oxidation was observed in fragments larger than b_{18}; this was indicative of H18 as a potential oxidation site. Fragments between b_{18} and b_{32}, however, appeared in both oxidized and nonoxidized forms, which suggested that there was another oxidation site apart from H18. In the spectrum of doubly oxidized hIAPP (Figure 6 e), no doubly oxidized ion was displayed other than the whole peptide itself, which possibly revealed that Y37 might be the second oxidation site.

Previous studies proposed that methionine, histidine, and tyrosine residues in amyloidogenic peptides were susceptible to oxidative modification, which could affect their aggregation behavior.[3e,h,j,15] Particularly, oxidative modifications of methionine residues have been reported to inhibit β-strand formation of amyloidogenic peptides.[3h,j,15] Incorporation of oxygen atoms into methionine residues could provide partial negative charges and further enhance the polarity of peptides.[3c,h,15] In the case of Aβ, the increased polarity of oxidized M35 could reduce hydrophobic contacts in the C-terminal region and destabilize a β-strand structure in which M35 proximately interacts with the aromatic ring of F19.[3h,15] Along with a change in polarity, greater structural disorder and reduced helicity were also found in methionine-oxidized α-Syn.[3c,16] Specifically, oxidation at M116 and M127 presumably disrupts α-Syn aggregation because these residues are suggested to mediate long-range interactions with the central hydrophobic regions.[17] Other important oxidation sites are histidine residues. Due to its structural features, such as an imidazole ring and two protonation states, histidine has versatile roles in multiple interactions (e.g., cationic–π interactions, π–π stacking, hydrogen–π interactions, coordination, and hydrogen bonding).[18] Depending on pH, histidine can present different protonation states that have effects on the molecular behavior of amyloidogenic peptides, including aggregation, through alteration of the strength of interactions.[18,19] In addition, histidine is known as a metal binding site in amyloidogenic peptides.[20] Binding of metal ions (e.g., Cu^{II}, Zn^{II}) to peptides is shown to accelerate amyloidogenic peptide aggregation or induce the formation and stabilization of toxic oligomeric aggregates.[1b,20b,c,21] Upon the formation of 2-oxo-histidine, metal binding affinities were reported to be substantially decreased; thus, oxidative modifications of histidine residues might destabilize complexes of amyloidogenic peptides with metal ions.[20e,22] Collectively, methionine, histidine, and/or tyrosine residues, the potential oxidation sites of Aβ, α-Syn, or hIAPP, which were suggested to be essential for the properties and aggregation of these amyloidogenic peptides, were indicated by our MS and NMR studies. Oxidative modifications are present at a few specific resi-
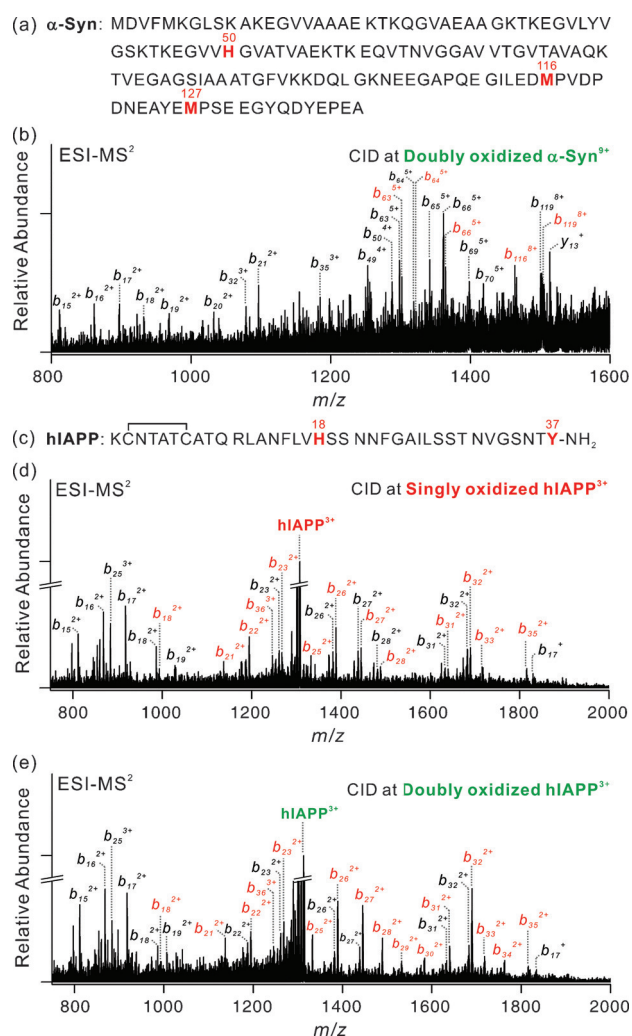

(a) α-Syn: MDVFMKGLSK AKEGVVAAAE KTKQGVAEAA GKTKEGVLYV GSKTKEGVV**H**50 GVATVAEKTK EQVTNVGGAV VTGVTAVAQK TVEGAGSIAA ATGFVKKDQL GKNEEGAPQE GILED**M**116PVDP DNEAYE**M**127PSE EGYQDYEPEA

(c) hIAPP: KCNTATCATQ RLANFLV**H**18SS NNFGAILSST NVGSNT**Y**37-NH$_2$

Figure 6. Identification of oxidation sites in α-Syn and hIAPP. Sequences of (a) α-Syn and (c) hIAPP. ESI-MS^2 spectra for (b) doubly oxidized α-Syn, and (d) singly and (e) doubly oxidized hIAPP. Nonoxidized, singly oxidized, and doubly oxidized fragments are indicated in black, red, and green, respectively.

dues in amyloidogenic peptides, which might be able to modulate their aggregation pathways potentially through altering intra- or intermolecular interactions critical for β-strand formation (see below).

Aggregation behavior influenced upon oxidation of amyloidogenic peptides by light-activated Ir-1

Changes in size distribution

To investigate whether peptide oxidation could transmute the aggregation of amyloidogenic peptides, two inhibition (Figure 7a and Figure S6a in the Supporting Information) and disaggregation (Figure S7a in the Supporting Information) experiments[2b–e] were carried out mainly with Aβ (two major isoforms, Aβ$_{40}$ and Aβ$_{42}$). Size distributions of the resultant Aβ$_{40}$ and Aβ$_{42}$ species treated with Ir-1 were evaluated by gel electrophoresis with Western blotting (gel/Western blot) by using an anti-Aβ antibody (6E10).

In the inhibition studies (Figure 7a), when fresh Aβ$_{40}$ was incubated with Ir-1 in the presence of light under aerobic conditions, various molecular weights (MWs) of peptide species were visualized in the gel/Western blot (Figure 7b, left). Distinct from the result with light exposure, Ir-1 could not generate diverse sizes of Aβ aggregates without light. In addition, when the ligands, 1 and 2-phenylquinoline (Figure 1b), were not coordinated to the Ir^{III} center, they had no noticeable effect on Aβ aggregation, even with light under aerobic conditions (Figure 7b and Figure S6 in the Supporting Information). When Ir-1 was incubated with fresh Aβ$_{42}$, similar reactivity trends were presented to those with Aβ$_{40}$ (Figure 7b, right). Diverse MW distributions of Aβ$_{42}$ species were shown with both Ir-1 and light. Furthermore, the inhibition experiments were conducted in the absence of O$_2$ to verify if Aβ aggregation could be influenced upon oxidation of peptides by oxidants generated by O$_2$ with light-activated Ir-1. Aβ aggregation pathways were not indicated to be varied under anaerobic conditions, even in the presence of light (Figure 7b, middle).

Moreover, in order to disassemble preformed Aβ$_{40}$ aggregates or redirect their further aggregation upon oxidation with Ir-1 in the presence of light and O$_2$, the disaggregation experiment was carried out (Figure S7 in the Supporting Information). Similar to the inhibition studies, preformed Aβ$_{40}$ aggregates were observed with a wide range of sizes only after treatment with Ir-1 upon light exposure in the presence of O$_2$. Overall, our gel/Western blot results from both inhibition and disaggregation experiments suggest that 1) Ir-1 is able to transmute Aβ aggregation pathways only with light activation under aerobic conditions; and 2) the overall structure of Ir-1 over individual structural components (e.g., ligand 1) is essential to alter Aβ aggregation in the presence of both light and O$_2$. Combining the results with the control of light and O$_2$, it is demonstrated that Aβ oxidation, triggered by photoactivated Ir-1 with O$_2$, could direct the modulation of peptide aggregation pathways.

Morphological changes of amyloidogenic peptides

The degree of regulating the aggregation pathways of amyloidogenic peptides was also monitored through morphological changes visualized by transmission electron microscopy (TEM) (Figure 7c and d). From the TEM analyses, the resultant peptides upon treatment with both Ir-1 and light under aerobic conditions were observed to be smaller, while either structured fibrils or large aggregates were indicated without light. In the case of Aβ$_{40}$, the treatment of the peptide with Ir-1 induced the formation of short and thin fibrils in the presence of both light and O$_2$ (Figure 7c). Additionally, the morphologies of α-Syn and hIAPP were also transformed to smaller amorphous aggregates when Ir-1 was added with exposure of both light and O$_2$, instead of large aggregates or fibrils produced in the absence of Ir-1 (Figure 7d). Therefore, along with the gel/Western blot data, our TEM studies imply that the aggregation of amyloidogenic peptides could be transfigured upon treatment with light-activated Ir-1 under aerobic conditions.
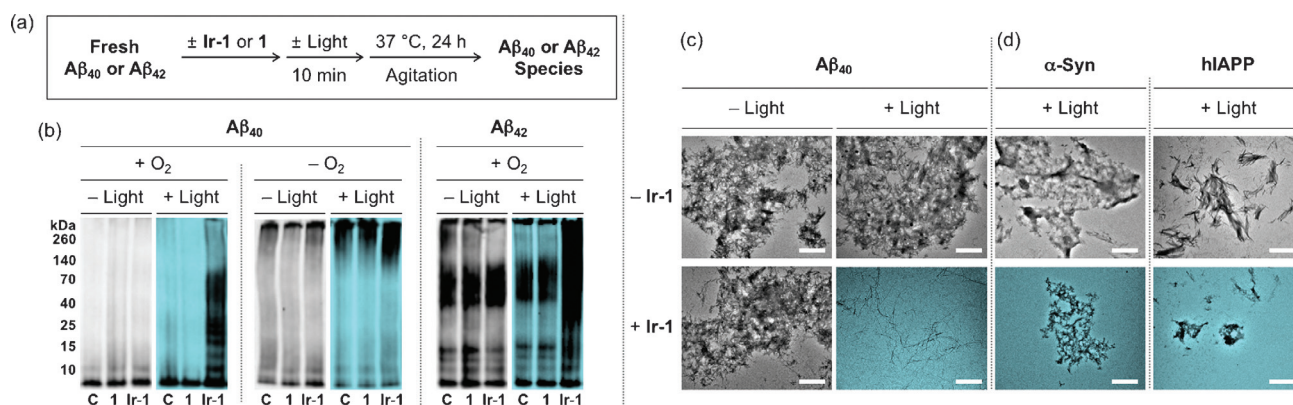

Figure 7. Effects of Ir-1 and 1 on peptide aggregation pathways. (a) Scheme of the inhibition experiments. (b) Analyses of the resultant Aβ$_{40}$ and Aβ$_{42}$ species generated from various conditions [aerobic (left) and anaerobic (right) conditions] by gel/Western blot with an anti-Aβ antibody (6E10). Lanes: (C) Aβ$_{40}$ or Aβ$_{42}$; (1) Aβ$_{40}$ or Aβ$_{42}$ + 1; (Ir-1) Aβ$_{40}$ or Aβ$_{42}$ + Ir-1. (c and d) TEM images of the samples from (b) and the light-treated samples containing α-Syn or hIAPP with and without Ir-1 (scale bar = 1 μm). Conditions: [peptide] = 25 μM; [Ir-1 or 1] = 50 μM; pH 7.4; 37°C; 24 h; constant agitation; 1 sun light for 10 min (for samples treated with light).

Conclusion

Several strategies for understanding and suppressing the aggregation of amyloidogenic peptides, found in amyloid-related disorders and suggested to be linked to their pathogenesis, have been developed. One of the tactics would be related to oxidative modifications of the amino acid residues essential for properties and aggregation behavior of peptides. For peptide oxidation toward amyloidogenic peptides, an inorganic complex, **Ir-1**, rationally designed to be a chemical tool that has a relatively stable framework and is capable of generating oxidants (e.g., $^1O_2$) from readily accessible O_2 simply upon photoactivation by using low-energy radiation.

On the basis of our biochemical and biophysical analyses, **Ir-1** is shown to significantly induce oxidative modifications of amyloidogenic peptides, such as Aβ, α-Syn, and hIAPP, followed by alteration of their aggregation pathways. Peptide oxidation by photoactivated **Ir-1** is more noticeable for amyloidogenic peptides over well-structured nonamyloidogenic peptides. By employing MS and NMR, the oxidation sites are indicated to be potentially located at methionine, histidine, and/or tyrosine residues in these amyloidogenic peptides. Through minor alterations at a few specific residues in peptides by using photoactivated **Ir-1** under mild conditions, their aggregation pathways can be modulated. Overall, our rational design and fundamental investigations of **Ir-1** demonstrate the promise of an inorganic complex in being developed as a chemical tool for oxidative modifications of amyloidogenic peptides and subsequent control of their aggregation. Such a tool will assist in advancing our fundamental understanding toward amyloidogenic peptides, as well as providing insight into the development of effective approaches for amyloid management.

Experimental Section

Materials and methods

All reagents were purchased from commercial suppliers and used as received, unless otherwise noted. Compound **1** (**1**=methyl 4-(dimethylamino)picolinate)[23] and the cyclometalated chloride-bridged Ir^{III} dimer ([Ir(C^N)$_2$(μ-Cl)$_2$])[24] were prepared by following previously reported procedures. The prepared **Ir-1** was characterized by NMR, FTIR, HRMS, and elemental analyzer on an Agilent 400-MR DD2 NMR spectrometer, Varian Cary 620/670 FTIR spectrometer (UNIST Central Research Facilities, Ulsan, Republic of Korea), Bruker maXis™ HD Ultra-high resolution Q-TOF LC MS/MS system (HRMS; The Cooperative Laboratory Center of Pukyong National University, Busan, Republic of Korea), and Thermo Flash 2000 (UNIST Central Research Facilities, Ulsan, Republic of Korea), respectively. Aβ$_{40}$ and Aβ$_{42}$ were purchased from Anygen (Aβ$_{40}$ = DAEFRHDSGYEVHHQKLVFFAEDVGSNKGAIIGLMVGGVV, Aβ$_{42}$ = DAEFRHDSGYEVHHQKLVFFAEDVGSNKGAIIGLMVGGVVIA; Nammyun, Jangseong-gun, Republic of Korea). α-Syn and hIAPP were obtained from Anaspec and Peptron, respectively [α-Syn = MDVFMKGLSKAKEGVVAAAEKTKQGVAEAAGKTKEGVLYVGSKTKEGVVHGVATVAEKTKEQVTNVGGAVVTGVTAVAQKTVEGAGSIAAATGFVKKDQLGKNEEGAPQEGILEDMPVDPDNEAYEMPSEEGYQDYEPEA (Fremont, CA, USA); hIAPP = KCNTATCATQRLANFLVHSSNNFGAILSSTNVGSN-

TY-NH$_2$ (Daejeon, Republic of Korea)]. Ubiquitin was purchased from Sigma Aldrich (ubiquitin = MQIFVKTLTGKTITLEVEPSDTIENVKAKIQDKEGIPPDQQRLIFAGKQLEDGRTLSDYNIQKESTLHLVLRLRGG; St. Louis, MO, USA). Double-distilled H$_2$O (ddH$_2$O) was obtained from a Milli-Q Direct 16 system (Merck KGaA, Darmstadt, Germany). Irradiation with 1 sun was obtained with a Newport IQE-200 solar simulator (Irvine, CA, USA). ESI-MS and IM-MS analyses were performed by using a Waters Synapt G2-Si quadrupole time-of-flight ion mobility mass spectrometer equipped with an ESI source (DGIST Center for Core Research Facilities, Daegu, Republic of Korea). NMR studies of Aβ with **Ir-1** were conducted on a Bruker Avance 600 MHz spectrometer equipped with a TCI triple-resonance inverse detection cryoprobe. The data was processed by using TOPSPIN 2.1 (Bruker) software and assignments were made by using SPARKY 3.1134 software. Anaerobic reactions were performed in a N$_2$-filled glove box (Korea Kiyon, Bucheon-si, Gyeonggi-do, Republic of Korea). TEM images were taken by using a JEOL JEM-1400 transmission electron microscope (UNIST Central Research Facilities, Ulsan, Republic of Korea). Photophysical properties were measured by using an Agilent Cary 100 UV/Vis spectrophotometer and a Varian Cary Eclipse fluorescence spectrophotometer (UNIST Central Research Facilities, Ulsan, Republic of Korea). Time-correlated single-photon counting (TCSPC) was performed for lifetime measurements with a Ti:sapphire laser Mira900 (Coherent, Santa Clara, CA, USA), monochromator Acton series SP-2150i (Princeton Instruments, Acton, MA, USA), and TCSPC module Pico-Harp 300 (PicoQuant, Berlin, Germany) together with MCP-PMT R3809U-59 (Hamamatsu, Shizuika-ken, Japan) and fitted by Pico-Quant FluoFit software (UNIST Central Research Facilities, Ulsan, Republic of Korea).

Synthesis of Ir-1

2-Phenylquinoline (680 mg, 3.3 mmol) was added to a solution of IrCl$_3$·nH$_2$O (500 mg, 1.7 mmol) in a mixture of 2-methoxyethanol and H$_2$O (3:1). The solution was heated at reflux under N$_2$ (g) for 24 h. After cooling to room temperature, brown precipitates were obtained by treatment with additional H$_2$O. The crude product (cyclometalated chloride-bridged Ir^{III} dimer, [Ir(C^N)$_2$(μ-Cl)$_2$]) was washed with hexanes and cold diethyl ether several times, dried, and used without further purification.[24] A mixture of the cyclometalated chloride-bridged Ir^{III} dimer (353 mg, 0.28 mmol), **1** (150 mg, 0.83 mmol), and Na$_2$CO$_3$ (294 mg, 2.8 mmol) was dissolved in 2-ethoxyethanol. The mixture was heated at reflux under N$_2$ (g) for 12 h. After cooling to room temperature, the solution was concentrated, followed by the addition of H$_2$O. The organic phase was extracted with CH$_2$Cl$_2$ three times. The collected organic solution was dried with Na$_2$SO$_4$ and the solvent was removed under reduced pressure. The crude materials were purified by column chromatography (SiO$_2$, 50:1 CH$_2$Cl$_2$/CH$_3$OH, R$_f$ = 0.6) to give the product as a red powder (340 mg, 80%). FTIR (neat): $\tilde{v}$=3057, 2021, 1608, 1516, 1437, 1381, 1338, 1163, 1028, 762 cm^{-1}; UV/Vis (H$_2$O): λ_{max} (ε) = 463 nm (5.78 ($\pm$ 0.12) $\times$ 10^3 M^{-1} cm^{-1}). ^{1}H NMR (400 MHz, CDCl$_3$): δ = 8.79 (d, J= 8.0 Hz, 1H), 8.13 (t, J=8.0 Hz, 1H), 8.07 (m, 3H), 7.92 (dd, J= 8.0 Hz, 1H), 7.80 (dd, J=8.0 Hz, 1H), 7.70 (dd, J=8.0 Hz, 1H), 7.67 (dd, J=8.0 Hz, 1H), 7.51 (m, 2H), 7.42 (d, J=8.0 Hz, 1H), 7.39 (ddd, 1H) 7.26 (ddd, 1H), 7.03 (m, 2H), 6.95 (m, 2H), 6.89 (dd, J=8.0 Hz, 1H), 6.72 (m, 1H), 6.60 (dt, J=6.8 Hz, 1H), 6.30 (m, 2H), 2.87 ppm (s, 6H); ^{13}C NMR (100 MHz, CDCl$_3$): δ = 173.0, 171.1, 169.2, 154.4, 151.8, 151.4, 148.7, 147.8, 147.0, 145.9, 145.1, 138.1, 136.3, 134.8, 129.4, 128.5, 126.0, 125.2, 121.5, 120.5, 116.1, 109.7, 108.8, 39.1 ppm; HRMS: m/z calcd for C$_{38}$H$_{29}$IrN$_4$NaO$_2$ [M+Na]$^+$: 789.1812; found: 789.1814; elemental analysis calcd (%) for

$C_{38}H_{29}IrN_4O_2 \cdot 0.5\,CH_3OH$: C 59.14, H 4.00, N 7.17; found: C 59.00, H 4.01, N 7.19.

Electrospray ionization ion mobility mass spectrometry (ESI-IM-MS)

$A\beta_{40}$, α-Syn, hIAPP, and ubiquitin (100 μм) were incubated with **Ir-1** or **1** (500 μм) in 100 mм ammonium acetate (pH 7.5) at 37 °C without any agitation. Incubated peptides were diluted 10-fold and then injected into a mass spectrometer. The capillary voltage, sampling cone voltage, and source temperature were set to 2.8 kV, 70 V, and 40 °C, respectively. The backing pressure was adjusted to 3.2 mbar. Ion mobility wave height and velocity were adjusted to 10 V and 450 m s^{-1}, respectively, and gas flow for the helium cell and ion mobility cell was set to 120 and 30 mL min^{-1}, respectively. Tandem MS (MS^2) analyses were additionally performed on the nonoxidized (Figure S8 in the Supporting Information) and singly/doubly oxidized peptides. The ESI parameters and experimental conditions were same as those reported above. Collision-induced dissociation was conducted by applying the collision energy in the trap and adjusting LM resolution to 15. More than 200 spectra were obtained for each sample and averaged for analyses. To estimate collision cross-section values for obtained IM-MS data, calibration was also performed by following previously reported procedures (Figure S9 in the Supporting Information).[25]

Mass spectrometric analyses

Oxidized $A\beta_{40}$, α-Syn, hIAPP, and ubiquitin were observed upon incubation with **Ir-1** under aerobic conditions in the presence of light by using a Waters Synapt G2-Si Q-ToF mass spectrometer equipped with an ESI source. Only major charge states of all peptides (+3 for $A\beta_{40}$ and hIAPP, +9 for α-Syn, and +5 for ubiquitin) were selected and shown in all mass spectra. Generally, exact mass should be calculated based on monoisotopic mass; however, in the present study, the oxidized peaks were assigned based on m/z values of the most abundant peaks because monoisotopic mass values of α-Syn could not be well resolved without a high-resolution mass spectrometer. For example, +3-charged $A\beta_{40}$ was most dominantly found in ESI-MS (Figure 2a). Upon treatment of **Ir-1** and light, the singly oxidized $A\beta_{40}$ ions were abundantly observed at 1449.6 m/z, corresponding to a 16 Da increase in mass from the nonoxidized $A\beta_{40}$ peak at 1444.2 m/z (Figure 2a, bottom; blue). In the case of +9-charged α-Syn at 1607.8 m/z, the singly oxidized peak was not well defined due to overlap with sodiated ions at 1610.2 m/z. With the treatment of **Ir-1** and light, doubly oxidized α-Syn was found at 1611.3 m/z, which indicated an approximate 32 Da increase in mass (Figure 2b, bottom; blue). The +3-charged hIAPP presented an oxidized peak at 1306.9 m/z, indicating a 14 Da difference in mass from nonoxidized ions with 1302.2 m/z upon treatment with **Ir-1** and light (Figure 2c, bottom; blue). Different from $A\beta_{40}$ and α-Syn, singly oxidized hIAPP indicated a 14 Da increase in mass. In the ESI-MS spectra of ubiquitin, the +5 charge state was most abundantly detected (Figure S4 in the Supporting Information). Singly and doubly oxidized ubiquitin were found at 1717.2 and 1720.3 m/z, respectively, which were approximately 16 and 32 Da increases in mass from nonoxidized ubiquitin centered at 1713.9 m/z (Figure S4 in the Supporting Information, bottom; blue).

[1] a) M. P. Lambert, A. K. Barlow, B. A. Chromy, C. Edwards, R. Freed, M. Liosatos, T. E. Morgan, I. Rozovsky, B. Trommer, K. L. Viola, P. Wals, C. Zhang, C. E. Finch, G. A. Krafft, W. L. Klein, *Proc. Natl. Acad. Sci. USA* **1998**, *95*, 6448 – 6453; b) M. G. Savelieff, A. S. DeToma, J. S. Derrick, M. H. Lim, *Acc. Chem. Res.* **2014**, *47*, 2475 – 2482; c) M. Baba, S. Nakajo, P.-H. Tu, T. Tomita, K. Nakaya, V. M.-Y. Lee, J. Q. Trojanowski, T. Iwatsubo, *Am. J. Pathol.* **1998**, *152*, 879 – 884; d) G. J. S. Cooper, B. Leighton, G. D. Dimitriadis, M. Parry-Billings, J. M. Kowalchuk, K. Howland, J. B. Rothbard, A. C. Willis, K. B. M. Reid, *Proc. Natl. Acad. Sci. USA* **1988**, *85*, 7763 – 7766; e) F. Chiti, C. M. Dobson, *Annu. Rev. Biochem.* **2006**, *75*, 333 – 366; f) D. M. Hartley, D. M. Walsh, C. P. Ye, T. Diehl, S. Vasquez, P. M. Vassilev, D. B. Teplow, D. J. Selkoe, *J. Neurosci.* **1999**, *19*, 8876 – 8884.

[2] a) S. I. A. Cohen, P. Arosio, J. Presto, F. R. Kurudenkandy, H. Biverstål, L. Dolfe, C. Dunning, X. Yang, B. Frohm, M. Vendruscolo, J. Johansson, C. M. Dobson, A. Fisahn, T. P. J. Knowles, S. Linse, *Nat. Struct. Mol. Biol.* **2015**, *22*, 207 – 213; b) S.-J. Hyung, A. S. DeToma, J. R. Brender, S. Lee, S. Vivekanandan, A. Kochi, J.-S. Choi, A. Ramamoorthy, B. T. Ruotolo, M. H. Lim, *Proc. Natl. Acad. Sci. USA* **2013**, *110*, 3743 – 3748; c) H. J. Lee, R. A. Kerr, K. J. Korshavn, J. Lee, J. Kang, A. Ramamoorthy, B. T. Ruotolo, M. H. Lim, *Inorg. Chem. Front.* **2016**, *3*, 381 – 392; d) J. S. Derrick, R. A. Kerr, Y. Nam, S. B. Oh, H. J. Lee, K. G. Earnest, N. Suh, K. L. Peck, M. Ozbil, K. J. Korshavn, A. Ramamoorthy, R. Prabhakar, E. J. Merino, J. Shearer, J.-Y. Lee, B. T. Ruotolo, M. H. Lim, *J. Am. Chem. Soc.* **2015**, *137*, 14785 – 14797; e) M. W. Beck, J. S. Derrick, R. A. Kerr, S. B. Oh, W. J. Cho, S. J. C. Lee, Y. Ji, J. Han, Z. A. Tehrani, N. Suh, S. Kim, S. D. Larsen, K. S. Kim, J.-Y. Lee, B. T. Ruotolo, M. H. Lim, *Nat. Commun.* **2016**, *7*, 13115; f) G. S. Yellol, J. G. Yellol, V. B. Kenche, X. M. Liu, K. J. Barnham, A. Donaire, C. Janiak, J. Ruiz, *Inorg. Chem.* **2015**, *54*, 470 – 475.

[3] a) A. Taniguchi, D. Sasaki, A. Shiohara, T. Iwatsubo, T. Tomita, Y. Sohma, M. Kanai, *Angew. Chem. Int. Ed.* **2014**, *53*, 1382 – 1385; *Angew. Chem.* **2014**, *126*, 1406 – 1409; b) M. Friedemann, E. Helk, A. Tiiman, K. Zovo, P. Palumaa, V. Tõugu, *Biochem. Biophys. Rep.* **2015**, *3*, 94 – 99; c) C. B. Glaser, G. Yamin, V. N. Uversky, A. L. Fink, *Biochim. Biophys. Acta* **2005**, *1703*, 157 – 169; d) W. Zhou, C. Long, S. H. Reaney, D. A. Di Monte, A. L. Fink, V. N. Uversky, *Biochim. Biophys. Acta* **2010**, *1802*, 322 – 330; e) V. N. Uversky, G. Yamin, P. O. Souillac, J. Goers, C. B. Glaser, A. L. Fink, *FEBS Lett.* **2002**, *517*, 239 – 244; f) M. Palmblad, A. Westlind-Danielsson, J. Bergquist, *J. Biol. Chem.* **2002**, *277*, 19506 – 19510; g) L. He, X. Wang, D. Zhu, C. Zhao, W. Du, *Metallomics* **2015**, *7*, 1562 – 1572; h) L. Hou, H. Shao, Y. Zhang, H. Li, N. K. Menon, E. B. Neuhaus, J. M. Brewer, I.-J. L. Byeon, D. G. Ray, M. P. Vitek, T. Iwashita, R. A. Makula, A. B. Przybyla, M. G. Zagorski, *J. Am. Chem. Soc.* **2004**, *126*, 1992 – 2005; i) L. Hou, I. Kang, R. E. Marchant, M. G. Zagorski, *J. Biol. Chem.* **2002**, *277*, 40173 – 40176; j) A. A. Watson, D. P. Fairlie, D. J. Craik, *Biochemistry* **1998**, *37*, 12700 – 12706; k) A. Taniguchi, Y. Shimizu, K. Oisaki, Y. Sohma, M. Kanai, *Nat. Chem.* **2016**, *8*, 974 – 982.

[4] a) S. R. Paik, H.-J. Shin, J.-H. Lee, *Arch. Biochem. Biophys.* **2000**, *378*, 269 – 277; b) S. Guedes, R. Vitorino, R. Domingues, F. Amado, P. Domingues,

Rapid Commun. Mass Spectrom. **2009**, *23*, 2307–2315; c) K. Inoue, C. Garner, B. L. Ackermann, T. Oe, I. A. Blair, *Rapid Commun. Mass Spectrom.* **2006**, *20*, 911–918; d) M. Pietruszka, E. Jankowska, T. Kowalik-Jankowska, Z. Szewczuk, M. Smużyńska, *Inorg. Chem.* **2011**, *50*, 7489–7499.

[5] a) M. C. DeRosa, R. J. Crutchley, *Coord. Chem. Rev.* **2002**, *233–234*, 351–371; b) M. Tomita, M. Irie, T. Ukita, *Biochemistry* **1969**, *8*, 5149–5160; c) H.-R. Shen, J. D. Spikes, C. J. Smith, J. Kopeček, *J. Photochem. Photobiol. A* **2000**, *130*, 1–6; d) V. V. Agon, W. A. Bubb, A. Wright, C. L. Hawkins, M. J. Davies, *Free Radic. Biol. Med.* **2006**, *40*, 698–710; e) K. Huvaere, L. H. Skibsted, *J. Am. Chem. Soc.* **2009**, *131*, 8049–8060; f) J. E. Plowman, S. Deb-Choudhury, A. J. Grosvenor, J. M. Dyer, *Photochem. Photobiol. Sci.* **2013**, *12*, 1960–1967; g) C. Castaño, E. Oliveros, A. H. Thomas, C. Lorente, *J. Photochem. Photobiol. B* **2015**, *153*, 483–489; h) B. I. Lee, S. Lee, Y. S. Suh, J. S. Lee, A.-k. Kim, O.-Y. Kwon, K. Yu, C. B. Park, *Angew. Chem. Int. Ed.* **2015**, *54*, 11472–11476; *Angew. Chem.* **2015**, *127*, 11634–11638; i) S.-y. Takizawa, R. Aboshi, S. Murata, *Photochem. Photobiol. Sci.* **2011**, *10*, 895–903; j) K. Kim, D. A. Fancy, D. Carney, T. Kodadek, *J. Am. Chem. Soc.* **1999**, *121*, 11896–11897; k) D. A. Fancy, C. Denison, K. Kim, Y. Xie, T. Holdeman, F. Amini, T. Kodadek, *Chem. Biol.* **2000**, *7*, 697–708; l) F. Amini, C. Denison, H.-J. Lin, L. Kuo, T. Kodadek, *Chem. Biol.* **2003**, *10*, 1115–1127; m) S. Meunier, E. Strable, M. G. Finn, *Chem. Biol.* **2004**, *11*, 319–326.

[6] a) E. Alarcón, A. M. Edwards, A. Aspee, C. D. Borsarelli, E. A. Lissi, *Photochem. Photobiol. Sci.* **2009**, *8*, 933–943; b) P. Drössler, W. Holzer, A. Penzkofer, P. Hegemann, *Chem. Phys.* **2003**, *286*, 409–420; c) E. Niu, K. P. Ghiggino, A. W.-H. Mau, W. H. F. Sasse, *J. Lumin.* **1988**, *40–41*, 563–564; d) J. A. Ferreira, R. Barral, J. D. Baptista, M. I. C. Ferreira, *J. Lumin.* **1991**, *48–49*, 385–390.

[7] J. S. Temenoff, H. Shin, P. S. Engel, A. G. Mikos, *Proc. Second Joint EMBS/BMES Conference* **2002**, 687–688.

[8] a) M. Yoshimura, M. Ono, H. Watanabe, H. Kimura, H. Saji, *Sci. Rep.* **2014**, *4*, 6155; b) C.-W. Lee, M.-P. Kung, C. Hou, H. F. Kung, *Nucl. Med. Biol.* **2003**, *30*, 573–580; c) Z. Liu, P. J. Sadler, *Acc. Chem. Res.* **2014**, *47*, 1174–1185; d) Y. You, *Curr. Opin. Chem. Biol.* **2013**, *17*, 699–707; e) M. S. Lowry, S. Bernhard, *Chem. Eur. J.* **2006**, *12*, 7970–7977; f) H.-J. Zhong, L. Lu, K.-H. Leung, C. C. L. Wong, C. Peng, S.-C. Yan, D.-L. Ma, Z. Cai, H.-M. D. Wang, C.-H. Leung, *Chem. Sci.* **2015**, *6*, 5400–5408; g) T.-S. Kang, Z. Mao, C.-T. Ng, M. Wang, W. Wang, C. Wang, S. M.-Y. Lee, Y. Wang, C.-H. Leung, D.-L. Ma, *J. Med. Chem.* **2016**, *59*, 4026–4031; h) N. Onishi, S. Xu, Y. Manaka, Y. Suna, W.-H. Wang, J. T. Muckerman, E. Fujita, Y. Himeda, *Inorg. Chem.* **2015**, *54*, 5114–5123.

[9] I.-S. Shin, J. I. Kim, T.-H. Kwon, J.-I. Hong, J.-K. Lee, H. Kim, *J. Phys. Chem. C* **2007**, *111*, 2280–2286.

[10] K. L. Schey, E. L. Finley, *Acc. Chem. Res.* **2000**, *33*, 299–306.

[11] F. Lanucara, S. W. Holman, C. J. Gray, C. E. Eyers, *Nat. Chem.* **2014**, *6*, 281–294.

[12] S. Vijay-Kumar, C. E. Bugg, W. J. Cook, *J. Mol. Biol.* **1987**, *194*, 531–544.

[13] V. H. Wysocki, K. A. Resing, Q. Zhang, G. Cheng, *Methods* **2005**, *35*, 211–222.

[14] C. Schöneich, T. D. Williams, *Chem. Res. Toxicol.* **2002**, *15*, 717–722.

[15] A. M. Brown, J. A. Lemkul, N. Schaum, D. R. Bevan, *Arch. Biochem. Biophys.* **2014**, *545*, 44–52.

[16] A. Binolfi, A. Limatola, S. Verzini, J. Kosten, F.-X. Theillet, H. M. Rose, B. Bekei, M. Stuiver, M. van Rossum, P. Selenko, *Nat. Commun.* **2016**, *7*, 10251.

[17] C. W. Bertoncini, Y.-S. Jung, C. O. Fernandez, W. Hoyer, C. Griesinger, T. M. Jovin, M. Zweckstetter, *Proc. Natl. Acad. Sci. USA* **2005**, *102*, 1430–1435.

[18] S.-M. Liao, Q.-S. Du, J.-Z. Meng, Z.-W. Pang, R.-B. Huang, *Chem. Cent. J.* **2013**, *7*, 44–55.

[19] K. Garai, C. Frieden, *Proc. Natl. Acad. Sci. USA* **2013**, *110*, 3321–3326.

[20] a) P. Faller, C. Hureau, *Dalton Trans.* **2009**, *7*, 1080–1094; b) R. M. Rasia, C. W. Bertoncini, D. Marsh, W. Hoyer, D. Cherny, M. Zweckstetter, C. Griesinger, T. M. Jovin, C. O. Fernández, *Proc. Natl. Acad. Sci. USA* **2005**, *102*, 4294–4299; c) A. A. Valiente-Gabioud, V. Torres-Monserrat, L. Molina-Rubino, A. Binolfi, C. Griesinger, C. O. Fernández, *J. Inorg. Biochem.* **2012**, *117*, 334–341; d) J. R. Brender, K. Hartman, R. P. R. Nanga, N. Popovych, R. de la Salud Bea, S. Vivekanandan, E. N. G. Marsh, A. Ramamoorthy, *J. Am. Chem. Soc.* **2010**, *132*, 8973–8983; e) C. Cheignon, P. Faller, D. Testemale, C. Hureau, F. Collin, *Metallomics* **2016**, *8*, 1081–1089.

[21] Y.-P. Yu, P. Lei, J. Hu, W.-H. Wu, Y.-F. Zhao, Y.-M. Li, *Chem. Commun.* **2010**, *46*, 6909–6911.

[22] D. A. K. Traoré, A. E. Ghazouani, L. Jacquamet, F. Borel, J.-L. Ferrer, D. Lascoux, J.-L. Ravanat, M. Jaquinod, G. Blondin, C. Caux-Thang, V. Duarte, J.-M. Latour, *Nat. Chem. Biol.* **2009**, *5*, 53–59.

[23] H. J. Bolink, E. Coronado, S. G. Santamaria, M. Sessolo, N. Evans, C. Klein, E. Baranoff, K. Kalyanasundaram, M. Graetzel, M. K. Nazeeruddin, *Chem. Commun.* **2007**, *31*, 3276–3278.

[24] M. Nonoyama, *Bull. Chem. Soc. Jpn.* **1974**, *47*, 767–768.

[25] B. T. Ruotolo, J. L. P. Benesch, A. M. Sandercock, S.-J. Hyung, C. V. Robinson, *Nat. Protoc.* **2008**, *3*, 1139–1152.